

3-23-2017

Tuning the Effective Anisotropy in a Voltage-Susceptible Exchange-Bias Heterosystem

Will Echtenkamp

University of Nebraska-Lincoln, s-wechten1@unl.edu

Mike Street

University of Nebraska - Lincoln, mstreet@huskers.unl.edu

Ather Mahmood

University of Nebraska - Lincoln, ather.mahmood@unl.edu

Christian Binek

University of Nebraska-Lincoln, cbinek@unl.edu

Follow this and additional works at: <http://digitalcommons.unl.edu/physicsbinek>

 Part of the [Condensed Matter Physics Commons](#)

Echtenkamp, Will; Street, Mike; Mahmood, Ather; and Binek, Christian, "Tuning the Effective Anisotropy in a Voltage-Susceptible Exchange-Bias Heterosystem" (2017). *Christian Binek Publications*. 88.
<http://digitalcommons.unl.edu/physicsbinek/88>

This Article is brought to you for free and open access by the Research Papers in Physics and Astronomy at DigitalCommons@University of Nebraska - Lincoln. It has been accepted for inclusion in Christian Binek Publications by an authorized administrator of DigitalCommons@University of Nebraska - Lincoln.

Tuning the Effective Anisotropy in a Voltage-Susceptible Exchange-Bias Heterosystem

Will Echtenkamp, Mike Street, Ather Mahmood, and Christian Binek

*Department of Physics and Astronomy and the Nebraska Center for Materials and Nanoscience,
University of Nebraska-Lincoln, Lincoln, Nebraska 68588, USA*

(Received 31 October 2016; revised manuscript received 9 February 2017; published 23 March 2017)

Voltage- and temperature-tuned ferromagnetic hysteresis is investigated by a superconducting quantum-interference device and Kerr magnetometry in a thin-film heterostructure of a perpendicular anisotropic Co/Pd ferromagnet exchange coupled to the magnetoelectric antiferromagnet Cr₂O₃. An abrupt disappearance of exchange bias with a simultaneous more than twofold increase in coercivity is observed and interpreted as a competition between the effective anisotropy of Cr₂O₃ and the exchange-coupling energy between boundary magnetization and the adjacent ferromagnet. The effective anisotropy energy is given by the intrinsic anisotropy energy density multiplied by the effective volume separated from the bulk through a horizontal antiferromagnetic domain boundary. Kerr measurements show that the anisotropy of the interfacial Cr₂O₃ can be tuned isothermally and in the absence of an external magnetic field by application of an electric field. A generalized Meiklejohn-Bean model accounts for the change in exchange bias and coercivity as well as the asymmetric evolution of the hysteresis loop. In support of this model, the reversal of the boundary magnetization is experimentally confirmed as a contribution to the magnetic hysteresis loop.

DOI: [10.1103/PhysRevApplied.7.034015](https://doi.org/10.1103/PhysRevApplied.7.034015)

I. INTRODUCTION

Direct electric control of magnetization is of vital importance to the continuing advancement of information technology. Energy-efficient, nonvolatile memory technologies, for example, have been proposed which exploit electric control of magnetization [1–3]. Currently, electric control of magnetization and particularly reversible 180° switching remains a scientific challenge. One promising route is voltage control of exchange bias where, in the case of complete bipolar exchange-bias switching, the remnant magnetization of the ferromagnet can be switched between positive and negative values near saturation. Exchange bias can arise when a thin-film ferromagnet is deposited on an antiferromagnet. The exchange coupling between the antiferromagnet and the ferromagnet has the effects of shifting the ferromagnetic hysteresis loop to one side along the magnetic field axis and increasing the ferromagnetic coercivity if loose interface spins are present. Voltage control of exchange bias has recently been achieved in Cr₂O₃- (chromia-) based magnetic heterostructures [4–10]. Chromia is antiferromagnetic and magnetoelectric, and these properties, when held simultaneously, give rise to a unique property known as boundary magnetization [11–17]. Boundary magnetization is an unconventional net magnetization at the boundary of antiferromagnetic magnetoelectrics. When a ferromagnetic thin film is deposited on the (0001) face of chromia, it is this boundary magnetization which exchange couples to the ferromagnet and causes exchange bias. The orientation of the boundary magnetization is determined by the domain state of chromia. Chromia has two degenerate 180° antiferromagnetic domains with

opposite boundary magnetizations. Importantly, the domain state of chromia can be selected isothermally by the simultaneous application of an electric and magnetic field. In doing so, the boundary magnetization, as well as the exchange bias can be changed from positive to negative values. These changes are nonvolatile and do not require dissipative electric currents. Voltage-controlled exchange bias can serve as a building block for energy-efficient and fast memory and logic devices. A prominent example is the implementation of Cr₂O₃ and related high- T_N alloys in a magnetoelectric magnetic random-access memory (MRAM) described in detail in Refs. [18–20]. An impressive room-temperature demonstration of a conceptually related chromia-based MRAM has recently been achieved by Kosub *et al.* [21]. Exchange coupling between the boundary magnetization and the ferromagnetic layer allows voltage control of the remnant magnetization, which serves as the state variable. This writing mechanism is energy efficient and inert against detrimental effects from Joule heating. In order to develop those device proposals into device demonstrations that can operate reliably in a CMOS environment of 85 °C, the physics of the voltage-controlled switching and the properties of heterostructures from magnetoelectric antiferromagnets and ferromagnetic films requires a better understanding. A unique temperature dependence of exchange bias sometimes arises in chromia-based heterostructures [22,23]. This temperature dependence causes the exchange bias to abruptly drop to zero, far below the Néel temperature T_N , which is the maximum temperature exchange bias can be expected. Losing exchange bias destroys every hope for a useful room-temperature device. To solve this problem, one

first has to understand it. This paper does just that, showing that the detrimental transition into zero exchange bias is a domain effect rather than an intrinsic material issue.

In the present work, we investigate this temperature dependence. We propose that the abrupt disappearance of the exchange bias can be explained by a competition between the exchange between the ferromagnet and the boundary magnetization and the anisotropy of the chromia. The transition to zero exchange bias occurs when it is energetically favorable for the boundary magnetization to rotate with the ferromagnet as the magnetic field is cycled. In addition to the abrupt disappearance of the exchange bias, this same effect also explains a dramatic enhancement to the coercivity of the hysteresis loop. We present a generalized Meiklejohn-Bean model, which incorporates the effect of a horizontal domain wall near the antiferromagnetic-ferromagnetic interface. The model utilizes the accompanying concept of an effective temperature-dependent antiferromagnetic layer thickness which, at the transition, reduces to the critical pinning thickness known from the conventional Meiklejohn-Bean pinning criterion. Finally, samples are exposed to electric fields which have the effect of isothermally triggering the transition to partial depinning.

II. SAMPLE FABRICATION

Two samples are fabricated using a combination of laser deposition and thermal evaporation. For sample 1, a sapphire substrate is cleaned using modified Radio Corporation of America protocol [24]. The substrate is introduced into an ultrahigh-vacuum chamber for chromium and palladium to be deposited by molecular beam epitaxy. A 1-nm chromium adhesion layer is grown at 300 °C. The palladium is grown according to a three-step growth process [25]. A seed layer of 7 nm is grown at 650 °C. The sample is then cooled to 50 °C, and an additional 50 nm of palladium is grown. Finally, the temperature is raised to 650 °C to crystallize the palladium. This process minimizes the roughness of the final film. The sample is then introduced into a separate vacuum chamber for deposition of chromia by pulsed laser deposition. A KrF excimer laser with pulse energies of 200 mJ and pulse width of 20 ns at a repetition rate of 10 Hz creates a plume from a chromia target, allowing deposition of (0001) textured chromia thin films on top of the palladium. The temperature of the substrate is maintained at 500 °C while a total of 500 nm is deposited. Finally, a perpendicular ferromagnetic film of Pd(1 nm) + [Co(0.6 nm)/Pd(1 nm)]₂ is deposited by molecular beam epitaxy while the sample is maintained at a temperature of 300 °C. Sample 2 is likewise prepared, except on the final step, a shadow mask is applied to the sample, restricting the Co/Pd deposition to the 300- μm^2 region.

III. EXPERIMENTAL RESULTS

The hysteresis loops for sample 1 are measured using a superconducting quantum-interference device. Figure 1 shows the evolution of the ferromagnetic hysteresis loops

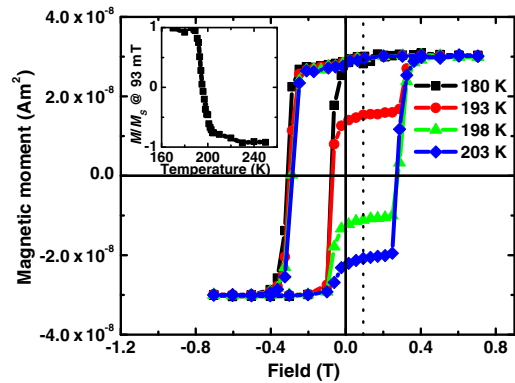


FIG. 1. Hysteresis loops of the magnetization of perpendicular anisotropic Co/Pd for temperatures 180 K (squares), 193 K (circles), 198 K (triangles), and 203 K (diamonds). Diamagnetic background from the substrate is subtracted. Inset: Relative magnetization (M/M_s^+ , magnetization/positive saturation magnetization) at 93 mT (dotted line in the main figure) during the ascending branch of the hysteresis loop.

and the associated exchange-bias effects as a function of the temperature. The initial sample state is prepared via field cooling from $T = 330$ K to $T = 170$ K in $B = 1$ T applied normal to the film, i.e., along the easy axes of both the ferromagnet and antiferromagnet. Below 180 K, the hysteresis is fully shifted to the left, with both the zero magnetization point of the descending branch (H_{C1}) and ascending branch (H_{C2}) having negative values. As the sample is heated, the ascending branch of the hysteresis loop undergoes a notable change. When applying the standard definition of the exchange-bias field according to $\mu_0 H_{EB} = \mu_0 (H_{C1} + H_{C2})/2$, the exchange bias decreases from nearly 200 mT at $T = 180$ K to zero at $T = 200$ K. This evolution is localized to the ascending branch of the hysteresis loop. The inset in Fig. 1 shows the relative magnetization [M/M_s^+ (magnetization/positive saturation magnetization)] at 93 mT (dotted line in the main figure) during the ascending branch of the hysteresis loop.

Figure 2 shows the absolute value of exchange bias as a function of the temperature and the coercive field $\mu_0 H_c = \mu_0 |H_{C2} - H_{C1}|/2$. The coercive field jumps up dramatically just as the exchange bias goes to zero. Note that this behavior is in strong contrast to most ordinary exchange-bias systems which do not possess boundary magnetization. The unusual increase in coercivity is a strong indication for dragging of boundary magnetization on reversal of the ferromagnet. The jump in both exchange bias and coercivity corresponds to the temperature at which the step in the ascending branch of the hysteresis loop descends below the zero magnetic moment axis.

IV. ANALYSIS AND DISCUSSION

The disappearance of exchange bias, doubling of coercivity, and apparent asymmetric evolution of the hysteresis loop can be understood by applying a coherent rotation

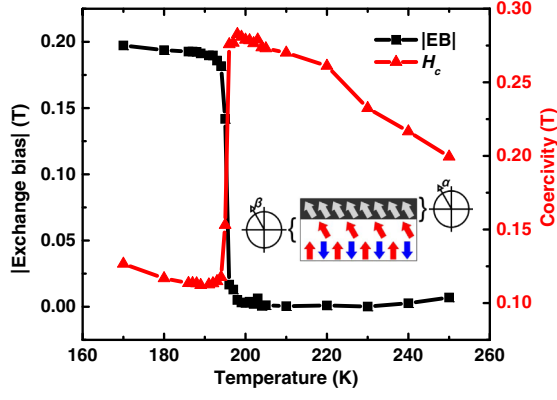


FIG. 2. Absolute value of the hysteresis loop's exchange bias (squares) and coercivity (triangles). Coercive fields are determined from interception with the magnetic field axis. The inset shows a schematic of the sample including a cartoon of the spin structure. Lower layer of up and down arrows depicts the antiferromagnetic order, the second layer depicts the boundary magnetization, and the top layer depicts the spins of the ferromagnet. Angles α and β are visualized relative to the common easy axis of the spins.

model to the antiferromagnetic ferromagnetic interface [26,27]. In such a system, one can write the total energy as

$$\begin{aligned}
 F = & -\mu_0 H M_{\text{FM}} t_{\text{FM}} \cos(\beta) - \mu_0 H M_{\text{AF}} t_{\text{AF}} \cos(\alpha) \\
 & + K_{\text{FM}} t_{\text{FM}} \sin^2(\beta) + K_{\text{AF}} t_{\text{AF}} \sin^2(\alpha) \\
 & - J S_{\text{FM}} S_{\text{AF}} \cos(\beta - \alpha),
 \end{aligned} \quad (1)$$

where M_{FM} , M_{AF} , t_{FM} , t_{AF} , K_{FM} , K_{AF} are the magnetizations, thicknesses, and anisotropy constants of the ferromagnet and antiferromagnet, respectively. S_{FM} and S_{AF} are the interface magnetizations of the ferromagnet and antiferromagnet, while J is the exchange constant which describes the coupling between them. β and α are the angles of the ferromagnetic and antiferromagnetic magnetizations, both interface and bulk, with respect to the uniaxial anisotropy easy axis which is aligned along the film normal. Fields are applied normal to the sample surface. The inset of Fig. 2 shows a schematic of the sample and its spin structure with the lower layer of arrows depicting the antiferromagnetic order, the second layer depicting the boundary magnetization, and the top layer depicting the spins of the ferromagnet. Angles α and β are visualized relative to the common easy axis of the spins.

The equilibrium behavior of the antiferromagnetic interface magnetization can be ascertained using

$$\begin{aligned}
 \frac{\partial F}{\partial \alpha} = 0 = & \mu_0 H M_{\text{AF}} t_{\text{AF}} \sin(\alpha) + 2K_{\text{AF}} t_{\text{AF}} \sin(\alpha) \cos(\alpha) \\
 & - J S_{\text{FM}} S_{\text{AF}} \sin(\beta - \alpha) \\
 \approx & 2K_{\text{AF}} t_{\text{AF}} \sin(\alpha) \cos(\alpha) - J S_{\text{FM}} S_{\text{AF}} \sin(\beta - \alpha).
 \end{aligned} \quad (2)$$

Here, the term containing M_{AF} is negligibly small, as we demonstrate later. As Meiklejohn points out, exchange bias can arise only if the anisotropy energy of the antiferromagnet is large compared to the exchange field [28]. Equation (2) can motivate the origin of Meiklejohn's criterion. It shows a crossover behavior as the antiferromagnetic anisotropy or exchange terms are varied. For $K_{\text{AF}} t_{\text{AF}} \gg J S_{\text{FM}} S_{\text{AF}}$, $\alpha \rightarrow 0$ implying a rigid antiferromagnet, while for $J S_{\text{FM}} S_{\text{AF}} \gg K_{\text{AF}} t_{\text{AF}}$, $\alpha \rightarrow \beta$ implying rotation of the antiferromagnetic interface magnetization in concert with the ferromagnet. The crossover happens at $K_{\text{AF}} t_{\text{AF}}^c = J S_{\text{AF}} S_{\text{FM}} / 2$ in accordance with Meiklejohn's criterion.

The extrema of the free energy can be found by solving in addition $\partial F / \partial \beta = 0$,

$$\begin{aligned}
 \frac{\partial F}{\partial \beta} = 0 = & \mu_0 H M_{\text{FM}} t_{\text{FM}} \sin(\beta) + 2K_{\text{FM}} t_{\text{FM}} \sin(\beta) \cos(\beta) \\
 & + J S_{\text{FM}} S_{\text{AF}} \sin(\beta - \alpha).
 \end{aligned} \quad (3)$$

For large anisotropy of the antiferromagnet, all spins of the antiferromagnet remain parallel to the c axis implying $\alpha \approx 0$. Therefore, in the limit of high anisotropy of the antiferromagnet, $(\partial F / \partial \beta) = 0$ can be simplified into

$$\begin{aligned}
 \frac{\partial F}{\partial \beta} = 0 = & \mu_0 H M_{\text{FM}} t_{\text{FM}} \sin(\beta) + 2K_{\text{FM}} t_{\text{FM}} \sin(\beta) \cos(\beta) \\
 & + J S_{\text{FM}} S_{\text{AF}} \sin(\beta),
 \end{aligned} \quad (4)$$

which yields

$$\cos(\beta) = -\frac{\mu_0 H M_{\text{FM}} t_{\text{FM}} + J S_{\text{FM}} S_{\text{AF}}}{2K_{\text{FM}} t_{\text{FM}}}. \quad (5)$$

Substituting Eq. 5 into

$$\begin{aligned}
 \frac{\partial^2 F}{\partial \beta^2} = & \mu_0 H M_{\text{FM}} t_{\text{FM}} \cos(\beta) + 2K_{\text{FM}} t_{\text{FM}} (2\cos^2 \beta - 1) \\
 & + J S_{\text{FM}} S_{\text{AF}} \cos(\beta)
 \end{aligned} \quad (6)$$

provides an expression for the curvature of the free energy. Switching of the magnetization happens when a local minimum becomes unstable such that the free energy has a horizontal tangent according to $(\partial^2 F / \partial \beta^2) = 0$. This condition yields the well-known Meiklejohn-Bean expression for exchange bias $\mu_0 H_{\text{EB}} = -J S_{\text{FM}} S_{\text{AF}} / M_{\text{FM}} t_{\text{FM}}$ from the coercive fields

$$\begin{aligned}
 \mu_0 H_{c1} = & \frac{-2K_{\text{FM}} t_{\text{FM}} - J S_{\text{FM}} S_{\text{AF}}}{M_{\text{FM}} t_{\text{FM}}}, \\
 \mu_0 H_{c2} = & \frac{2K_{\text{FM}} t_{\text{FM}} - J S_{\text{FM}} S_{\text{AF}}}{M_{\text{FM}} t_{\text{FM}}}.
 \end{aligned} \quad (7)$$

However, if instead it is assumed that the anisotropy of the antiferromagnet is small, the exchange between the

ferromagnet and antiferromagnet interface magnetization is large enough to couple them together so that the spins of both the ferromagnet and the antiferromagnet coherently rotate in the external magnetic field. In this limit, where $\alpha = \beta$, the free energy simplifies as

$$F^* = -\mu_0 H M_{\text{FM}} t_{\text{FM}} \cos(\beta) - \mu_0 H M_{\text{AF}} t_{\text{AF}} \cos(\beta) + K_{\text{FM}} t_{\text{FM}} \sin^2(\beta) + K_{\text{AF}} t_{\text{AF}} \sin^2(\beta) - J S_{\text{FM}} S_{\text{AF}}. \quad (8)$$

Using the same procedure as above, one obtains $\mu_0 H_{\text{EB}} = 0$ from the coercive fields

$$\begin{aligned} \mu_0 H_{c1}^* &= -\frac{2(K_{\text{FM}} t_{\text{FM}} + K_{\text{AF}} t_{\text{AF}})}{M_{\text{FM}} t_{\text{FM}} + M_{\text{AF}} t_{\text{AF}}}, \\ \mu_0 H_{c2}^* &= +\frac{2(K_{\text{FM}} t_{\text{FM}} + K_{\text{AF}} t_{\text{AF}})}{M_{\text{FM}} t_{\text{FM}} + M_{\text{AF}} t_{\text{AF}}}. \end{aligned} \quad (9)$$

For temperatures below 180 K, the data shown in Fig. 2 imply that the former condition of Eq. (7) is approximately satisfied, and the boundary magnetization remains fixed. For temperatures above 220 K, the latter condition of Eq. (9) is satisfied, and the boundary magnetization rotates with the ferromagnet.

In the present case, the chromia film is 500 nm thick, far above the minimum critical thickness necessary for exchange bias. Therefore, implicit in the assumption that the boundary magnetization rotates along with the ferromagnet is that the boundary magnetization becomes incommensurate with the underlying spin structure of the chromia by forming a horizontal domain wall. A boundary magnetization which is incommensurate with the domain state of the chromia has previously been used to describe electrically controlled exchange-bias training in a chromia-based heterostructure [6]. The onset of this depinning effect is given by the condition

$$K_{\text{AF}} t_{\text{AF}}^c = \frac{J S_{\text{AF}} S_{\text{FM}}}{2}. \quad (10)$$

Here, t_{AF}^c is the thickness of the chromia domain at the interface which reverses with the ferromagnet. In contrast to the simple Meiklejohn-Bean model where domains are not considered, here, t_{AF}^c is given by the temperature-dependent effective thickness of the horizontal antiferromagnetic domain rather than the geometrical film thickness. The effective anisotropy energy per area $K_{\text{AF}} t_{\text{AF}}^c$ is the intrinsic anisotropy energy density K_{AF} multiplied by the effective critical thickness t_{AF}^c determined by the distance between the interface and the horizontal antiferromagnetic domain boundary parallel to the interface. This interpretation is strongly supported by Ref. [29], which shows via continuous spin Monte Carlo simulation that horizontal antiferromagnetic domains are expected in chromia and that the temperature dependence of the domain-wall width of the horizontal domains has the

peculiar property to increase with decreasing temperature. This result supports our interpretation that the increase of an effective volume with decreasing temperature gives rise to the presence of exchange bias at temperatures below 180-K.

The above discussion suggests that a surplus moment originating from the boundary magnetization contributes to the saturation magnetization of the ferromagnetic hysteresis for temperatures above 180 K. In fact, the expected additional magnetic moment of the interface magnetization of the chromia rotating with the ferromagnet is evidenced by measuring the total change in magnetic moment (Δm) from positive magnetic saturation to negative magnetic saturation. Figure 3 shows Δm as a function of the temperature for the same sample, which generates the data for Figs. 1 and 2. Because the Δm effect is small and at the limit of resolution of the magnetometer, we ensure reproducibility with the help of another sample. Those data are shown in the inset of Fig. 3. The fact that the transition of this sample takes place slightly shifted with respect to the transition temperature of sample 1 is in strong support of the interpretation that the effect is based on domain formation with an intrinsic element of randomness. The Δm vs T data in the main panel of Fig. 3 show that in the same temperature region in which the hysteresis loop changes from negative to zero exchange bias (vertical lines in Fig. 3), Δm reverses the downward trend as the additional magnetic moment of the chromia interface spins begin to reverse with the ferromagnet. Figure 3 shows the additional change in magnetic moment due to the reversal of the boundary magnetization is approximately $7.5 \times 10^{-10} \text{ Am}^2$; one-half of this value is the total magnetic moment of the boundary magnetization (m_{AF}). So $M_{\text{AF}} t_{\text{AF}}^c = m_{\text{AF}} t_{\text{AF}}^c / (\text{area} \times t_{\text{AF}}^c)$, the area of the sample is $1.51 \times 10^{-5} \text{ m}^2$, so $M_{\text{AF}} t_{\text{AF}}^c = 2.5 \times 10^{-5} \text{ A}$. Likewise, $M_{\text{FM}} t_{\text{FM}} = 2.0 \times 10^{-3} \text{ A}$. Therefore, the following approximation is justified:

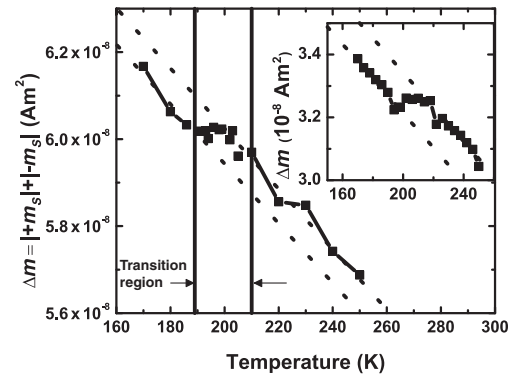


FIG. 3. Total change in the magnetic moment between positive and negative saturation magnetization as a function of the temperature. The transition region is marked. Dotted lines are to guide the eye. Inset shows data of a second piece of the same sample measured with identical protocol.

$$M_{\text{FM}}t_{\text{FM}} \gg M_{\text{AF}}t_{\text{AF}}^c. \quad (11)$$

This assertion is further verified by the lack of change in the descending branch of the hysteresis. Before the transition, $\mu_0 H_{c1} = (-2K_{\text{FM}}t_{\text{FM}} - JS_{\text{FM}}S_{\text{AF}})/(M_{\text{FM}}t_{\text{FM}})$. After the transition, using $K_{\text{AF}}t_{\text{AF}}^c = JS_{\text{FM}}S_{\text{AF}}/2$, the coercive field is $\mu_0 H_{c1}^* = (-2K_{\text{FM}}t_{\text{FM}} - JS_{\text{FM}}S_{\text{AF}})/(M_{\text{FM}}t_{\text{FM}} + M_{\text{AF}}t_{\text{AF}})$. As the temperature dependence of the descending branch in Fig. 1 shows no transition, the additional term in the denominator must be inconsequential.

Using Eq. (9) as well as Meiklejohn's critical thickness condition, the coercive fields of the hysteresis loop simplify to

$$\begin{aligned} \mu_0 H_{c1}^* &\approx \frac{-2K_{\text{FM}}t_{\text{FM}} - JS_{\text{AF}}S_{\text{FM}}}{M_{\text{FM}}t_{\text{FM}}}, \\ \mu_0 H_{c2}^* &\approx + \frac{2K_{\text{FM}}t_{\text{FM}} + JS_{\text{AF}}S_{\text{FM}}}{M_{\text{FM}}t_{\text{FM}}}. \end{aligned} \quad (12)$$

There are two things of note here. First, $\mu_0 H_{c1}^* = -\mu_0 H_{c2}^*$, which is the definition of a hysteresis with zero exchange bias. Second, $\mu_0 H_{c1}^* = \mu_0 H_{c1}$, while $\mu_0 H_{c2}^* \neq \mu_0 H_{c2}$, which explains the increase of the coercivity from $\mu_0 H_c = 2K_{\text{FM}}t_{\text{FM}}/M_{\text{FM}}t_{\text{FM}}$ to $\mu_0 H_c^* = (2K_{\text{FM}}t_{\text{FM}} + JS_{\text{AF}}S_{\text{FM}})/(M_{\text{FM}}t_{\text{FM}})$ solely due to change in the coercive field of the ascending branch.

Finally, the effective anisotropy of the chromium oxide can be altered isothermally by the application of electric and magnetic fields. As previously reported, by applying electric and magnetic fields across chromia, one of two degenerate 180° antiferromagnetic domains can be selected [5,6,9]. This effect has recently been shown in a thin-film system [4]. In the present case, the maximum electric field applied across the thin film is not sufficient to completely reverse the spin structure of the chromia, but it is sufficient to either reinforce or destabilize the region of chromia near the interface. The magneto-optical Kerr effect is used to examine the hysteresis of sample 2, and the experimental setup is described elsewhere [30]. Figure 4(a) shows the hysteresis loop of sample 2 at 295 K immediately after -12 V (squares), 0 V (triangles), and $+12$ V (circles) are applied simultaneously with -829 -mT magnetic field for approximately 1 s. In Fig. 4(b), the active portion of the loop is shown in more detail. The small steps in the hysteresis show that in some areas of the sample, the chromia does not rotate with the ferromagnet and causes exchange bias. In most areas, the sample is unpinned, and the chromia rotates with the ferromagnet. Those areas, which are pinned, show negative exchange bias. A chromia-ferromagnet heterostructure which exhibits negative exchange bias can be isothermally switched to positive exchange bias by applying a large enough positive field product. The squares in Fig. 4(b) show the result immediately after pulsing the positive field product of -829 mT and -12 V. The field is

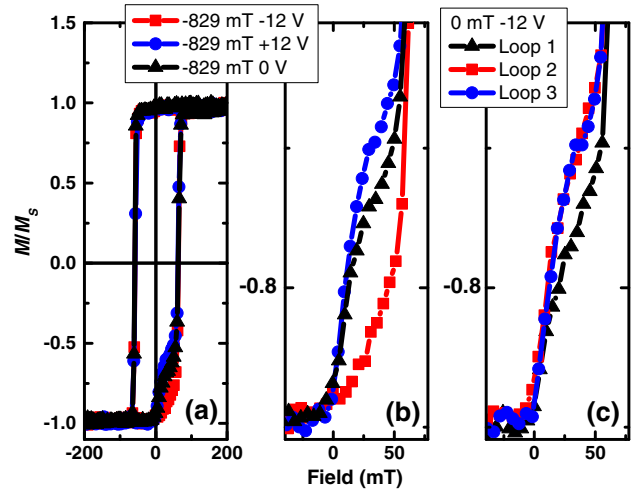


FIG. 4. (a) Hysteresis of sample 2 at 295 K after -829 -mT and $+12$ -V, 0 -V and -12 -V pulses. (b) Detail of the active region shown in (a). (c) Detail of the active region after 0 mT and -12 V is pulsed. Loops are taken in succession; each loop is measured in 50 s.

not sufficient to create positive exchange bias, but it does destabilize those areas, which are pinned to a negative exchange bias. By reversing the electric field, the effect is reversed. The circles in Fig. 4(b) show the effect after pulsing $+12$ V and -829 mT. This causes some chromia domains which, prior to field exposure, rotate with the ferromagnet to no longer rotate. This increase in the antiferromagnetic domain volume partially reinforces pinning of the ferromagnet and, thus, raises the step in the ascending branch. It should be noted that the effect is not persistent; after one reversal of the ferromagnet, the hysteresis loop reverts to its original state before any electric fields are applied.

Finally, it is possible to trigger this effect even without an external magnetic field. The active region in the chromia in this case is just below the interface to a depth of the critical thickness. In this region, the exchange field from the adjacent ferromagnet acts as an effective magnetic field. In Fig. 4(c), -12 V is pulsed with zero external magnetic field, while a negative remnant magnetization is maintained for the ferromagnet. The triangles show the hysteresis loop immediately after pulsing the electric field. The voltage pulse alone also has a destabilizing effect on those areas, which remain pinned, moving the step in the hysteresis loop lower. Figure 4(c) also shows the effect is not persistent, as the second (squares) and third (circles) loops after the pulse is applied return to their prepulse state. This finding has encouraging implications for the implementation of the converse magnetoelectric effect in device applications where the reversal of a magnetic layer can induce a voltage pulse. The results of Fig. 4 imply that within a certain penetration depth the exchange field of an adjacent ferromagnet mimics an applied magnetic field.

A magnetoelectric material responds with polarization on an applied magnetic field. Therefore, one can also expect polarization in response to the exchange field. Fast reversal of the ferromagnet and, thus, fast change of the exchange field give rise to fast change of the induced polarization in the adjacent magnetoelectric. This polarization change can be detected as a voltage pulse and used, e.g., as an alternative readout scheme replacing the frequently proposed approach via tunneling magnetoresistance in various spintronic devices.

In conclusion, we show that an effective anisotropy energy can be tuned by electrical means in the magnetoelectric antiferromagnet chromia. Effective anisotropy is the result of voltage-dependent formation of horizontal domains in proximity of the interface between chromia and an adjacent exchange-coupled ferromagnet. We argue that the abrupt disappearing of exchange bias of the ferromagnetic layer sets in when the horizontal domain thickness is less than the critical thickness for pinning. At this point, chromia's boundary magnetization reverses in concert with the magnetization reversal of the exchange-coupled ferromagnet. The lack of pinning due to subcritical effective anisotropy energy of the antiferromagnet also explains, in the framework of a generalized Meiklejohn-Bean model, the more than twofold increase of the coercivity at the transition. Our findings have important implications for the optimization of voltage-controlled exchange-bias heterostructures which are the building blocks for energy-efficient memory and logic device applications.

ACKNOWLEDGMENTS

This project is supported by the Nanoelectronics Research Corporation, a wholly owned subsidiary of the Semiconductor Research Corporation (SRC), through the Center for Nanoferroic Devices, a SRC-NRI Nanoelectronics Research Initiative Center under Tasks ID No. 2398.001 and No. 2587.001, by C-SPIN, one of six centers of STARnet, a SRC program sponsored by MARCO and DARPA, and by NSF through Nebraska Grant No. MRSEC DMR-1420645. The research is performed in part in the Nebraska Nanoscale Facility, Nebraska Center for Materials and Nanoscience, which is supported by the National Science Foundation under Grant No. NNCI:1542182, and the Nebraska Research Initiative.

-
- [1] C. Binek and B. Doudin, Magnetoelectronics with magnetoelectrics, *J. Phys. Condens. Matter* **17**, L39 (2005).
 - [2] W. Kleemann and C. Binek, in *Magnetic Nanostructures*, edited by H. Zabel and M. Farle (Springer Berlin, 2013), p. 163.
 - [3] P. A. Dowben, C. Binek, and D. E. Nikonov, in *Nanoscale Silicon Devices*, edited by S. Oda and D. K. Ferry (CRC Press, Boca Raton, FL, 2015).

- [4] P. Borisov, A. Hochstrat, X. Chen, W. Kleemann, and C. Binek, Magnetoelectric Switching of Exchange Bias, *Phys. Rev. Lett.* **94**, 117203 (2005).
- [5] X. He, Y. Wang, N. Wu, A. N. Caruso, E. Vescovo, K. D. Belashchenko, P. A. Dowben, and C. Binek, Robust isothermal electric control of exchange bias at room temperature, *Nat. Mater.* **9**, 579 (2010).
- [6] W. Echtenkamp and C. Binek, Electric Control of Exchange Bias Training, *Phys. Rev. Lett.* **111**, 187204 (2013).
- [7] S. M. Wu, S. A. Cybart, D. Yi, J. M. Parker, R. Ramesh, and R. C. Dynes, Full Electric Control of Exchange Bias, *Phys. Rev. Lett.* **110**, 067202 (2013).
- [8] J. T. Heron *et al.*, Deterministic switching of ferromagnetism at room temperature using an electric field, *Nature (London)* **516**, 370 (2014).
- [9] T. Ashida, M. Oida, N. Shimomura, T. Nozaki, T. Shibata, and M. Sahashi, Isothermal electric switching of magnetization in Cr₂O₃/Co thin film system, *Appl. Phys. Lett.* **106**, 132407 (2015).
- [10] K. Toyoki, Y. Shiratsuchi, A. Kobane, C. Mitsumata, Y. Kotani, T. Nakamura, and R. Nakatani, Magnetoelectric switching of perpendicular exchange bias in Pt/Co/ α -Cr₂O₃/Pt stacked films, *Appl. Phys. Lett.* **106**, 162404 (2015).
- [11] A. F. Andreev, Macroscopic magnetic fields of antiferromagnets, *J. Exp. Theor. Phys. Lett.* **63**, 758 (1996).
- [12] K. D. Belashchenko, Equilibrium Magnetization at the Boundary of a Magnetoelectric Antiferromagnet, *Phys. Rev. Lett.* **105**, 147204 (2010).
- [13] N. Wu, X. He, A. L. Wysocki, U. Lanke, T. Komesu, K. D. Belashchenko, C. Binek, and P. A. Dowben, Imaging and Control of Surface Magnetization Domains in a Magnetoelectric Antiferromagnet, *Phys. Rev. Lett.* **106**, 087202 (2011).
- [14] C. Shi *et al.*, Spin polarization asymmetry at the surface of chromia, *New J. Phys.* **16**, 073021 (2014).
- [15] L. Fallarino, C. Binek, and A. Berger, Boundary magnetization properties of epitaxial Cr_{2-x}Al_xO₃ thin films, *Phys. Rev. B* **91**, 214403 (2015).
- [16] T. Kosub, M. Kopte, F. Radu, O. G. Schmidt, and D. Makarov, All-Electric Access to the Magnetic-Field-Invariant Magnetization of Antiferromagnets, *Phys. Rev. Lett.* **115**, 097201 (2015).
- [17] P. Borisov, T. Ashida, T. Nozaki, M. Sahashi, and D. Lederman, Magnetoelectric properties of 500-nm Cr₂O₃ films, *Phys. Rev. B* **93**, 174415 (2016).
- [18] M. Street, W. Echtenkamp, T. Komesu, S. Cao, P. A. Dowben, and C. Binek, Increasing the Néel temperature of magnetoelectric chromia for voltage-controlled spintronics, *Appl. Phys. Lett.* **104**, 222402 (2014).
- [19] P. Dowben, C. Binek, and D. Nikonov, in *Nanoscale Silicon Devices* (CRC Press, Boca Raton, FL, 2015), p. 255.
- [20] Z. Zhao, W. Echtenkamp, M. Street, C. Binek, and J.-P. Wang, Magnetoelectric device feasibility demonstration voltage control of exchange bias in perpendicular Cr₂O₃ Hall bar device, in *Proceedings of the 74th Annual Device Research Conference (DRC)* (IEEE, 2016).
- [21] T. Kosub *et al.*, Purely antiferromagnetic magnetoelectric random access memory, *Nat. Commun.* **8**, 13985 (2017).

- [22] S. Yu, F. Toshiaki, O. Hiroto, N. Hayato, and N. Ryoichi, High perpendicular exchange bias with a unique temperature dependence in Pt/Co/ α -Cr₂O₃ (0001) thin films, *Appl. Phys. Express* **3**, 113001 (2010).
- [23] S. Yu, T. Yuichiro, T. Kentaro, N. Yuuta, O. Satoshi, M. Chiharu, and N. Ryoichi, High-temperature regeneration of perpendicular exchange bias in a Pt/Co/Pt/ α -Cr₂O₃/Pt thin film system, *Appl. Phys. Express* **6**, 123004 (2013).
- [24] D. Zhang, Y. Wang, and Y. Gan, Characterization of critically cleaned sapphire single-crystal substrates by atomic force microscopy, XPS and contact angle measurements, *Appl. Surf. Sci.* **274**, 405 (2013).
- [25] T. Wagner, G. Richter, and M. Rühle, Epitaxy of Pd thin films on (100) SrTiO₃: A three-step growth process, *J. Appl. Phys.* **89**, 2606 (2001).
- [26] C. Binek, A. Hochstrat, and W. Kleemann, Exchange bias in a generalized Meiklejohn-Bean approach, *J. Magn. Magn. Mater.* **234**, 353 (2001).
- [27] C. Binek, Ising-type antiferromagnets—Model systems in statistical physics and in the magnetism of exchange bias, *Springer Tracts Mod. Phys.* **196**, 1 (2003).
- [28] W.H. Meiklejohn, Exchange anisotropy—A review, *J. Appl. Phys.* **33**, 1328 (1962).
- [29] R. Ahmed and R. H. Victora, Modeling temperature dependent exchange bias in systems with magnetoelectric chromia, *AIP Adv.* **7**, 055817 (2017).
- [30] S. Polisetty, J. Scheffler, S. Sahoo, Y. Wang, T. Mukherjee, X. He, and C. Binek, Optimization of magneto-optical Kerr setup: Analyzing experimental assemblies using Jones matrix formalism, *Rev. Sci. Instrum.* **79**, 055107 (2008).